The Plant Cell, Vol. 28: 426–438, February 2016, www.plantcell.org © 2016 American Society of Plant Biologists. All rights reserved.

The Nuclear Ribonucleoprotein SmD1 Interplays with Splicing, RNA Quality Control, and Posttranscriptional Gene Silencing in Arabidopsis[OPEN]

Emilie Elvira-Matelot,[a,1] Florian Bardou,[b,1] Federico Ariel,[b] Vincent Jauvion,[a] Nathalie Bouteiller,[a] Ivan Le Masson,[a] Jun Cao,[c,2] Martin D. Crespi,[b,3] and Hervé Vaucheret[a,3]

[a] Institut Jean-Pierre Bourgin, INRA, AgroParisTech, CNRS, Université Paris-Saclay, 78026 Versailles Cedex, France
[b] Institute of Plant Sciences Paris-Saclay (IPS2), CNRS, INRA, Universités Paris-Sud, Evry, Paris-Diderot, Sorbonne Paris-Cité, Université Paris-Saclay, 91405 Orsay, France
[c] Department of Molecular Biology, Max Planck Institute for Developmental Biology, D-72076 Tübingen, Germany

ORCID ID: 0000-0002-4017-6436 (E.E.-M.)

RNA quality control (RQC) eliminates aberrant RNAs based on their atypical structure, whereas posttranscriptional gene silencing (PTGS) eliminates both aberrant and functional RNAs through the sequence-specific action of short interfering RNAs (siRNAs). The *Arabidopsis thaliana* mutant *smd1b* was identified in a genetic screen for PTGS deficiency, revealing the involvement of SmD1, a component of the Smith (Sm) complex, in PTGS. The *smd1a* and *smd1b* single mutants are viable, but the *smd1a smd1b* double mutant is embryo-lethal, indicating that SmD1 function is essential. SmD1b resides in nucleoli and nucleoplasmic speckles, colocalizing with the splicing-related factor SR34. Consistent with this, the *smd1b* mutant exhibits intron retention at certain endogenous mRNAs. SmD1 binds to RNAs transcribed from silenced transgenes but not nonsilenced ones, indicating a direct role in PTGS. Yet, mutations in the RQC factors UPFRAMESHIFT3, EXORIBONUCLEASE2 (XRN2), XRN3, and XRN4 restore PTGS in *smd1b*, indicating that SmD1 is not essential for but rather facilitates PTGS. Moreover, the *smd1b mtr4* double mutant is embryo-lethal, suggesting that SmD1 is essential for mRNA TRANSPORT REGULATOR4-dependent RQC. These results indicate that SmD1 interplays with splicing, RQC, and PTGS. We propose that SmD1 facilitates PTGS by protecting transgene-derived aberrant RNAs from degradation by RQC in the nucleus, allowing sufficient amounts to enter cytoplasmic siRNA bodies to activate PTGS.

INTRODUCTION

Posttranscriptional gene silencing (PTGS) controls a wide diversity of processes in eukaryotes through mRNA degradation mediated by small 21- to 22-nucleotide short interfering RNAs (siRNAs) (Baulcombe, 2004; Voinnet, 2009; Martínez de Alba et al., 2013). PTGS starts with the production of double-stranded RNAs (dsRNAs) and their processing into siRNAs. These small siRNAs trigger the sequence-specific cleavage of mRNAs containing complementary sequences. When PTGS is induced by viral or transgenic RNAs, siRNAs target the degradation of the invading RNAs but also of homologous endogenous mRNAs, if any. A forward genetic screen based on the transgenic *Arabidopsis thaliana* line *L1*, which carries a posttranscriptionally silent *p35S:GUS* sense transgene, identified ~50 PTGS-deficient mutants that defined 12 independent *SUPPRESSOR OF GENE SILENCING* (*SGS*) loci. Mutations in these 12 *SGS* loci also impair PTGS in line *2a3*, which carries a *p35S:NIA2* sense transgene that triggers cosuppression of the endogenous genes *NIA1* and *NIA2.* A forward genetic screen directly based on line *2a3* identified three additional loci (*SGS13*, *SGS14*, and *SGS15*) required for 2a3 but not L1 silencing (Jauvion et al., 2010). So far, SGS2/RDR6, SGS3, SGS4/AGO1, SGS5/HEN1, SGS6/MET1, SGS7/SDE5, SGS8/JMJ14, SGS9/HPR1, and SGS13/SDE3 have been characterized (Elmayan et al., 1998; Fagard et al., 2000; Mourrain et al., 2000; Morel et al., 2002; Boutet et al., 2003; Jauvion et al., 2010; Le Masson et al., 2012). During PTGS triggered by sense transgenes (S-PTGS), primary siRNAs are produced from an aberrant RNA (Parent et al., 2015), methylated at their 3′ end by the methyltransferase HEN1 (HUA ENCHANCER1) (Boutet et al., 2003; Li et al., 2005) before loading into AGO1 (ARGONAUTE1), which cleaves complementary target RNAs (Morel et al., 2002; Baumberger and Baulcombe, 2005). AGO1-mediated cleavage generates RNA fragments that escape degradation due to the protective activity of SGS3 and are transformed into dsRNA by RDR6 (RNA-DEPENDENT-RNA-POLYMERASE6; Mourrain et al., 2000). These dsRNA are processed into siRNA duplexes by DICER-LIKE4 to produce secondary siRNAs. These secondary siRNAs are also loaded onto AGO1, which cleaves complementary transgene mRNAs, resulting in an amplification loop that reinforces silencing. MET1 and JMJ14 encode a DNA methyltransferase and a histone demethylase, respectively, which likely play a role in remodeling chromatin to allow the transcription of transgene-derived aberrant RNAs that induce

[1] These authors contributed equally to this work.
[2] Current address: Dow AgroSciences, Indianapolis, IN 46268.
[3] Address correspondence to martin.crespi@ips2.université-paris-saclay.fr or herve.vaucheret@versailles.inra.fr.
The author responsible for distribution of materials integral to the findings presented in this article in accordance with the policy described in the Instructions for Authors (www.plantcell.org) is: Hervé Vaucheret (herve.vaucheret@versailles.inra.fr).
[OPEN]Articles can be viewed online without a subscription.
www.plantcell.org/cgi/doi/10.1105/tpc.15.01045

PTGS (Le Masson et al., 2012). Also, SDE5 and HPR1 encode RNA trafficking proteins, which likely play a role in bringing RNA molecules at the right place during PTGS (Hernandez-Pinzon et al., 2007; Jauvion et al., 2010; Yelina et al., 2010).

Components of RNA processing complexes that counteract PTGS also have been identified. Known endogenous PTGS suppressors include 5′→3′ EXORIBONUCLEASE2 (XRN2), XRN3, XRN4, and their regulator FIERY1 (Gazzani et al., 2004; Gy et al., 2007); exosome components HEN2, mRNA TRANSPORT REGULATOR4 (MTR4), RIBOSOMAL RNA PROCESSING4 (RRP4), RRP6L1, RRP41, RRP44a, and SUPERKILLER3 (Moreno et al., 2013; Lange et al., 2014; Yu et al., 2015); decapping components DECAPPING1 (DCP1), DCP2, and VARICOSE (Thran et al., 2012; Martínez de Alba et al., 2015); nonsense-mediated decay components UPFRAMESHIFT1 (UPF1) and UPF3 (Moreno et al., 2013); and 3′ end processing factors ENHANCED SILENCING PHENOTYPE1 (ESP1), ESP4, ESP5, CARBONE CATABOLITE REPRESSOR4a, and 3′→5′ POLY(A)-SPECIFIC RIBONUCLEASE (Herr et al., 2006; Moreno et al., 2013). This revealed the diversity of RNA regulation processes intertwined with siRNA-mediated PTGS in all types of compartments (nucleolus, nucleoplasm, and cytoplasm). Likely, a tug of war between RNA quality control and RNA silencing contributes to determine the final transcriptome of the cell by addressing aberrant RNAs to one or the other degradation pathway. However, cellular factors that influence the partitioning of aberrant RNAs to one or the other pathway remain unknown.

Here, we show that the PTGS-defective mutant *sgs14* recovered from a genetic screen based on the *p35S:NIA2* sense transgene carries a deletion of the *SmD1b* gene, which encodes one of the two orthologs of the yeast Sm domain-containing protein SmD1, a small nuclear ribonucleoprotein of the conserved Smith (Sm) complex (Wang and Brendel, 2004). The Sm group of proteins was named after Stephanie Smith, the first patient in which the systemic lupus erythematosus-associated anti-Sm autoimmune antibodies were identified. Sm proteins are highly conserved among protists, fungi, animals, and plants and can be classified in several groups. A first group comprises the canonical proteins SmB, SmD1, SmD2, SmD3, SmE, SmF, and SmG; a second group comprises related LSM proteins LSM1 to LSM8. SmB/D1/D2/D3/E/F/G form the core particles of the U1, U2, U4, and U5 spliceosomal ribonucleoproteins, while LSM2-8 is part of the U6 small nuclear ribonucleoprotein also involved in pre-mRNA splicing. LSM1-7 proteins form a different complex, which participates in mRNA decapping in cytoplasmic processing bodies (P-bodies). Additional components (up to LSM16) play various roles, including maturation of U3 small nucleolar RNA, participation in the U7 ribonucleoprotein involved in the maturation of histone mRNA, degradation of mRNA precursors in the nucleus, mRNA translational control, and formation of P-bodies (Golisz et al., 2013, and references therein). The Arabidopsis genome contains 42 Sm and LSM genes (Cao et al., 2011), among which very few have been characterized (Perea-Resa et al., 2012; Golisz et al., 2013). In particular, the role of Arabidopsis SmD1 identified here is not known, although its implication in splicing could be suspected based on the function of yeast SmD1 in this process (Zhang et al., 2001). As we report here, localization studies revealed that Arabidopsis SmD1b colocalizes with the splicing-related factor SR34 in nuclear speckles. Consistent with this, the *smd1b* mutation affects the splicing of several endogenous mRNAs. Arabidopsis SmD1b also binds to RNAs transcribed from silenced transgenes but not nonsilenced ones, indicating a connection between splicing and PTGS. Nevertheless, PTGS is restored in *smd1b upf3*, *smd1b xrn2*, *smd1b xrn3*, and *smd1b xrn4* double mutants, indicating that SmD1b is not essential for PTGS. Moreover, *smd1b mtr4* mutants are not viable, indicating that SmD1b also participates to RQC, at least MTR4-dependent RQC. Together, these results indicate that SmD1 influences splicing and the partitioning of aberrant RNAs between RNA quality control and RNA silencing pathways, revealing a broad role of SmD1 in the regulation of gene expression.

RESULTS

SGS14 Encodes an Ortholog of Yeast SmD1

The *SGS14* locus is defined by a unique mutant allele, which was identified in a screen for PTGS-deficient mutants using the *2a3* line, which carries a transgene consisting of the *NIA2* gene under the control of the 35S promoter (Elmayan et al., 1998). In addition to PTGS deficiency, this mutant exhibits developmental defects, including reduced stature, leaf serration, and early flowering (Figures 1A and 1B). The *sgs14* mutation was mapped to a 164-kb interval on chromosome 4. Whole-genome sequencing revealed that fast-neutron mutagenesis had induced a deletion in this interval, removing six protein-coding genes (At4g02800, At4g02810, At4g02820, At4g02830, At4g02840, and At4g02850). Mutant lines harboring T-DNA insertions in the open reading frames of At4g02800, At4g02810, At4g02820, At4g02830, and At4g02850 did not exhibit developmental defects, suggesting that deletion of At4g02840 was responsible for the developmental defects of the *sgs14* mutants. However, the only available mutant in this gene had an insertion upstream of the open reading frame and did not exhibit developmental defects. Therefore, we transformed the *sgs14* mutant with a 6-kb genomic fragment carrying the At4g02840 gene. Because At4g02840 is one of the two Arabidopsis genes encoding a protein homologous to yeast SmD1 (Wang and Brendel, 2004), this 6-kb genomic fragment is referred to as *pSmD1b:SmD1b* in Figure 1C. At first, we transformed *sgs14* mutant plants from which the *2a3* locus has been segregated away. Among 40 *sgs14*/*pSmD1b:SmD1b* transformants, 39 developed like wild-type plants with regards to stature, leaf shape, and flowering time (Figure 1C), indicating that the deletion of At4g02840 is responsible for the developmental defects of the *sgs14* deletion mutant. However, because the deletion removed six adjacent genes, PTGS deficiency could be due to the deletion of any of the six genes and not related to the developmental defect observed. Thus, we also transformed *sgs14* mutant plants carrying the *2a3* locus. Among 86 *2a3*/*sgs14*/*pSmD1b:SmD1b* transformants, 84 exhibited *NIA2* cosuppression, i.e., they died within the first 2 weeks of growth, indicating that the deletion of At4g02840 is responsible for both developmental defects and PTGS-deficiency in the *sgs14* mutant, hereafter referred to as *smd1b.*

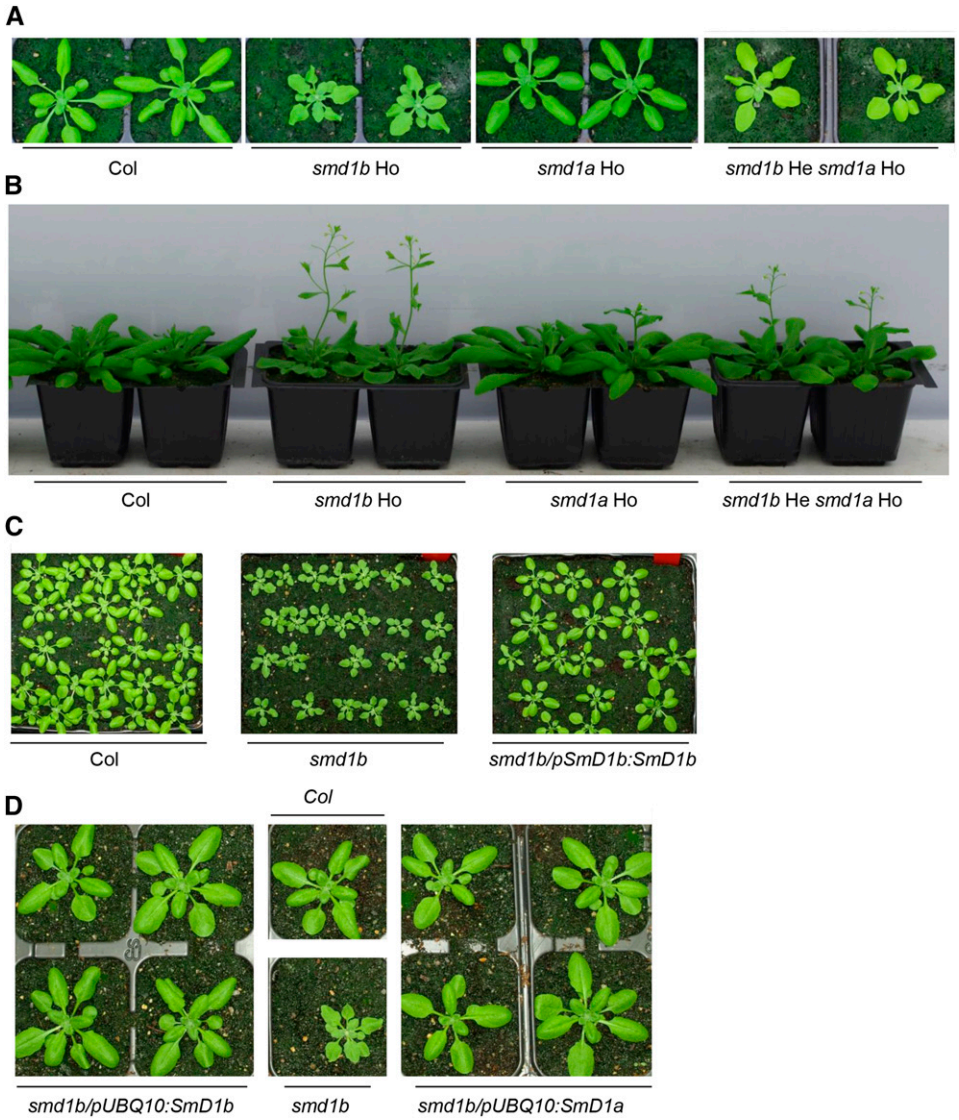

Figure 1. Developmental Defects of *smd1* Mutants.

(A) Photographs of 20-d-old plants of wild-type Col, *smd1a* and *smd1b* single mutants, and plants homozygous for *smd1a* and heterozygous for *smd1b*. Note that plants homozygous for *smd1b* and heterozygous for *smd1a*, or homozygous for both *smd1a* and *smd1b* are not viable.
(B) Photographs of 30-d-old plants of the same genotype as in **(A)**.
(C) Photographs of 20-d-old plants of wild-type Col, *smd1b* mutant, and *smd1b/pSmD1b:SmD1b* transformants.
(D) Photographs of 20-d-old plants of wild-type Col, *smd1b* mutant, and *smd1b/pUBQ10:SmD1a* and *smd1b/pUBQ10:SmD1b* transformants.

SmD1a and SmD1b Encode Redundant Proteins That Are Essential for Plant Viability

Yeast SmD1 has two orthologs in Arabidopsis, At3g07590 and At4g02840, which are referred to as SmD1a and SmD1b, respectively (Wang and Brendel, 2004). These two proteins only differ by 11 amino acids (Figure 2 A), suggesting that they could play redundant roles. Many T-DNA insertion lines exist around the *SmD1a* gene, but only SALK_024397 corresponds to an *smd1a* null allele (Figure 2B). Homozygous *smd1a* plants did not show any developmental defects when grown under standard laboratory conditions, raising questions about the functionality of this protein. However, both *pUBQ10:SmD1a-GFP* and *pUBQ10:SmD1b-GFP* constructs restored wild-type development and *NIA2* PTGS when introduced in *smd1b* or *2a3/smd1b* plants, respectively (Figure 1D), indicating that these two proteins have similar function. Analysis of expression arrays revealed that *SmD1b* mRNA accumulates at a higher level than *SmD1a* mRNA in wild-type plants (Figure 2C). Therefore, the absence of obvious developmental defects in the *smd1a* single mutant is likely due to the minor contribution of the *SmD1a* gene to the total amount of the SmD1 protein present in the cell. Supporting this hypothesis, *smd1a/smd1a smd1b/SmD1b* plants identified in the F2 progeny

deriving from a cross between *smd1a* and *smd1b* single mutants were viable and exhibited developmental defects milder than those of the *smd1b* mutant (Figures 1A and 1B), whereas *smd1a/SmD1a smd1b/smd1b* or *smd1a/smd1a smd1b/smd1b* plants could not be identified, suggesting that SmD1 function is essential and that the minimum level of protein needed for development requires either one copy of *SmD1b* or two copies of *SmD1a*. Accordingly, siliques formed on *smd1a/SmD1a smd1b/smd1b* plants lacked 25% of the seeds, indicating that the *smd1a/smd1a smd1b/smd1b* double mutant is embryo-lethal.

SmD1b Has Dual Localization in Nucleoli and Nuclear Speckles

We explored where SmD1a and SmD1b are expressed in the cell using transgenic *smd1b* mutants complemented with either the *pUBQ10:SmD1a-GFP* or *pUBQ10:SmD1b-GFP* construct. Confocal analysis revealed an exclusive nuclear localization of both fusion proteins (Figures 3A and 3B). Interestingly, two specific subnuclear localizations were observed. Indeed, SmD1b-GFP localized in both nucleoli and nucleoplasmic dots (Figure 3C). Nucleolar localization was confirmed by colocalization experiments using the nucleolar RQC factors UPF3 and XRN2 (Figures 3D and 3E). The nature of the nucleoplasmic dots was further analyzed using the splicing-related factor SR34, which resides in nucleoplasmic speckles (Lorković et al., 2008). Coinfiltration of *pUBQ10:SmD1b-GFP* and *p35S:SR34-RFP* indicated that SmD1b and SR34 colocalize in these speckles (Figure 3F).

The Splicing of Endogenous mRNAs Is Affected in *smd1b* Mutants

In yeast, the Sm proteins SmB, SmD1, and SmD3 make direct contact with the 5′ splice sites of pre-mRNA substrates and act by stabilizing RNA-RNA interactions between the 5′ end of the U1 small nuclear RNA and the 5′-splice sites (Zhang et al., 2001). The

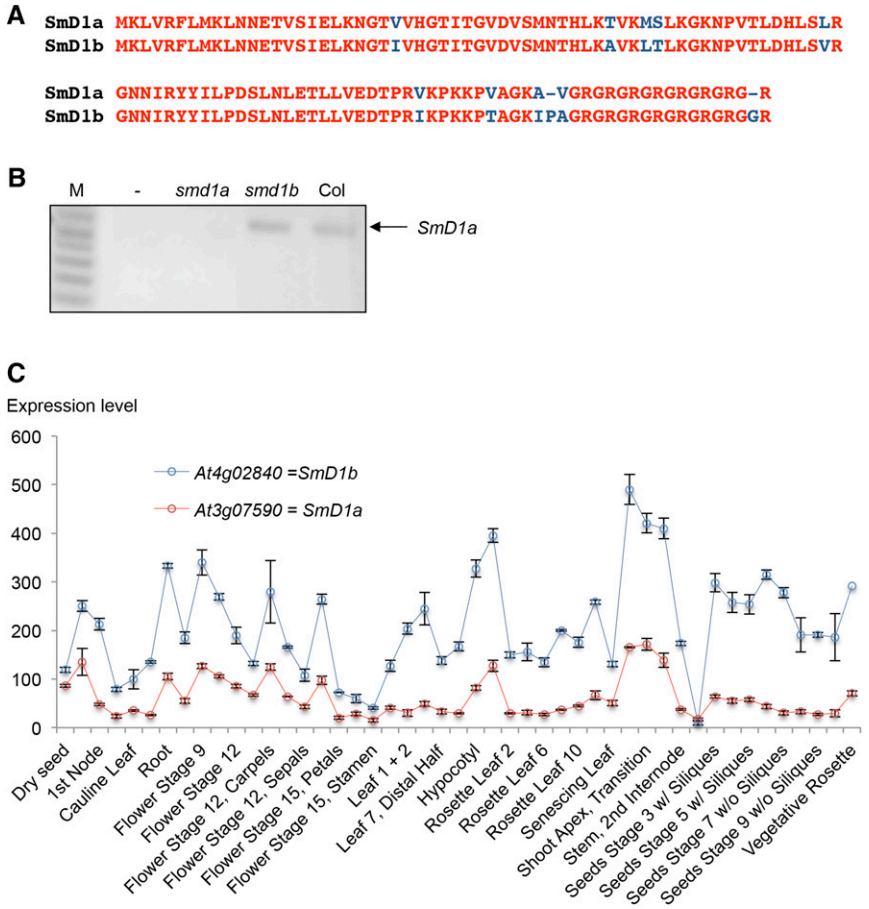

Figure 2. SmD1 Protein Sequence and *SmD1* Expression Patterns.

(A) Alignment of SmD1a and SmD1b proteins. Conserved amino acids are indicated in red.
(B) RT-PCR detection of *SmD1a* mRNA in wild-type (Col), *smd1b* (*sgs14*), and *smd1a* (SALK_024397) plants. M, molecular markers.
(C) ATH1 array expression profiles of *SmD1a* and *SmD1b* genes. Expression data were retrieved from the Arabidopsis eFP Browser. The expression of each *SmD1* gene is shown at various developmental stages and in different tissues. Normalization methods, the tissue, and the developmental stages of each sample as well as additional information can be found at http://bar.utoronto.ca/efp/cgi-bin/efpWeb.cgi?.

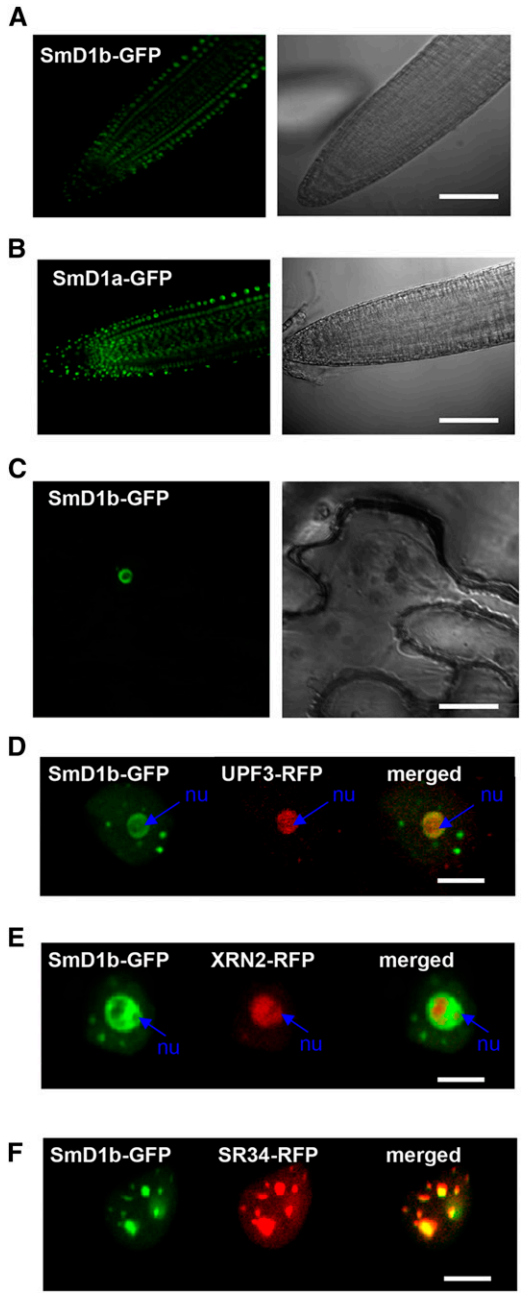

Figure 3. Subcellular Localization of SmD1 Proteins.

(A) and **(B)** Confocal images of Arabidopsis root expressing *pUBQ10:SmD1b-GFP* **(A)** or *pUBQ10:SmD1a-GFP* **(B)** reveal a nuclear localization. **(C)** Confocal image of *Nicotiana benthamiana* leaf infiltrated with *pUBQ10:SmD1b-GFP* reveal a localization in nucleoli and nucleoplasmic speckles. **(D)** and **(E)** Confocal images of *N. benthamiana* leaves infiltrated with *pUBQ10:SmD1b-GFP* and *pUBQ10:UPF3-RFP* **(D)** or *pUBQ10:XRN2-RFP* **(E)** reveal colocalization of the two proteins in the nucleolus (nu). **(F)** Confocal image of *N. benthamiana* leaf infiltrated with *pUBQ10:SmD1b-GFP* and *pUBQ10:SR34-RFP* reveal a localization in nucleoplasmic speckles.
Bars = 100 μm in **(A)** and **(B)**, 10 μm in **(C)**, and 5 μm in **(D)** to **(F)**.

role of yeast SmD1 in pre-mRNA splicing and the colocalization of Arabidopsis SmD1b with the splicing-related factor SR34 in nuclear speckles therefore suggest that Arabidopsis SmD1b could play a role in splicing. To test this hypothesis, the expression of genes known to produce alternatively spliced transcripts (Simpson et al., 2008) was analyzed in the *smd1a* and *smd1b* mutants. The auxin-related gene At2g33830 and the ATPase-encoding gene At1g27770 each transcribe a major isoform resulting from full splicing and a minor isoform resulting from intron retention. A higher accumulation of the intron-containing isoform of these two genes was observed in the *smd1b* mutant compared with Col (Figure 4). No change in the isoform ratio was observed in the *smd1a* mutant, confirming that SmD1b plays a more important role in splicing regulation than SmD1a.

SmD1 Does Not Participate in the Endogenous Small RNA Repertoire

Because many of the PTGS-deficient mutants previously identified in our screen are impaired in components of the cellular machinery producing endogenous siRNAs (Elmayan et al., 1998; Fagard et al., 2000; Mourrain et al., 2000; Morel et al., 2002; Boutet et al., 2003; Jauvion et al., 2010; Le Masson et al., 2012), we examined the accumulation of representative endogenous small RNAs in *smd1* mutants. The accumulation of microRNAs (miR173 and miR390), *trans*-acting siRNAs (TAS1, TAS2, and TAS3), and p4-siRNAs (siRNA02 and siRNA1003) was not affected in the *smd1a* or *smd1b* mutants (Figure 5), suggesting that SmD1 does not generally participate in the production of small RNAs but likely affects transgene PTGS at a different step.

The Effect of *smd1b* on Transgene PTGS Is Not Specific to Intron-Containing Transgenes but Rather Depends on the Strength of the Silencing Locus

The genetic screen that allowed recovering the *smd1b* mutant is based on the *2a3* line, which carries a silenced *35S:NIA2* transgene. At each generation, 10% of *2a3/smd1b* plants eventually trigger cosuppression of *NIA2* (Figure 6A), indicating that the *smd1b* mutation does not protect against *NIA2* cosuppression with 100% efficiency. To further characterize the effect of the *smd1b* mutation at the molecular level, high and low molecular weight RNAs were extracted from wild-type Col, *2a3* silenced plants, and *2a3/smd1b* and *2a3/sgs3* mutants and hybridized with a *NIA2* probe. *2a3/sgs3* mutants were used as a control because the *sgs3* mutation completely abolishes *NIA2* cosuppression triggered by the *2a3* locus (Mourrain et al., 2000). Whereas *2a3* plants accumulated *NIA2* siRNAs, *2a3/smd1b* mutants lacked *NIA2* siRNAs, similar to *2a3/sgs3* mutants (Figure 6B). However, *2a3/smd1b* mutants accumulated *NIA2* mRNA at a lower level than *2a3/sgs3* mutants (Figures 6B and 6C), consistent with the incomplete erasure of PTGS by the *smd1b* mutation (Figure 6A).

The *smd1b* mutant was not recovered in the PTGS genetic screen based on the *L1* line, which carries a silenced *p35S:GUS* transgene, although the *L1*-based screen identified a much larger number of PTGS-deficient mutants than the *2a3*-based screen. To test if *smd1b* has an effect on *L1* PTGS, the *L1* locus was introduced into *smd1b* by crossing. Unlike *2a3/smd1b* plants, which escaped *NIA2*

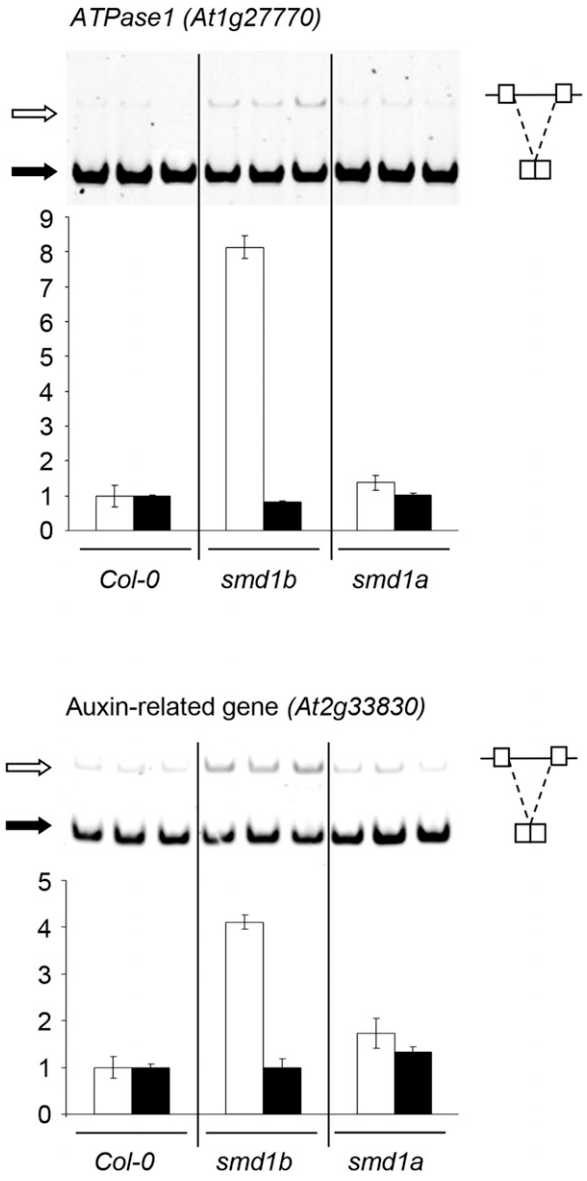

Figure 4. Endogenous RNA Accumulation in *smd1* Mutants.

RT-PCR and quantification of RNA isoforms of the *ATPase1* gene *At1g27770* and auxin-related gene *At2g33830* on PAGE gels. Black and white arrows indicate spliced and unspliced RNA, respectively. Increased intron retention is observed in *smd1b* but not *smd1a*.

cosuppression with 90% efficiency (Figure 6A), none of the *L1/smd1b* plants escaped *GUS* PTGS (Figure 6A). Indeed, *L1/smd1b* plants lacked *GUS* mRNA, similar to *L1* controls (Figure 6E). Nevertheless, *L1/smd1b* plants accumulated *GUS* siRNAs at a lower level than *L1* plants (Figure 6E), indicating that the *smd1b* mutation has an effect on *GUS* PTGS, although weaker than its effect on *NIA2* PTGS. Whether the *smd1a smd1b* double mutation could abolish *GUS* PTGS in *L1* could not be tested because of the lethality of this double mutant.

The *L1* and *2a3* loci differ by many aspects (genomic insertion site of the transgene, sequence of the mature mRNA, and presence or absence of an intron within the pre-mRNA). To determine the basis of the different behavior of the *smd1b* mutation toward *L1* and *2a3*, additional transgene loci were tested, including intron-containing and intron-free *p35S:GUS* loci. At first, the *159* locus was introduced into the *smd1b* mutant by crossing. The *159* locus carries the same *p35S:GUS* transgene as *L1* except for the presence of a plant intron within the *GUS* sequence (Vancanneyt et al., 1990). Like *L1*, line *159* exhibits high GUS activity at early stages of development, low GUS activity at later stages in 100% of the population (Figure 6A), and accumulates high levels of *GUS* siRNAs when PTGS is triggered (Figure 6F). However, the timing of silencing in line *159* is delayed compared with *L1*, indicating that the *159* locus is a weaker silencing inducer than the *L1* locus. Sixty-nine percent of *159/smd1b* plants escaped *GUS* PTGS and lacked GUS siRNAs, whereas 100% of *159/sgs3* plants escaped *GUS* PTGS (Figure 6A). Consistent with this, GUS activity and *GUS* mRNA levels in *159/smd1b* plants were high compared with *159* controls, although lower than in a *159/sgs3* plants (Figures 6F and 6G), confirming that *smd1b* incompletely suppresses PTGS.

Because the *2a3* and *159* loci carry intron-containing transgenes, whereas the *L1* locus carries an intron-free

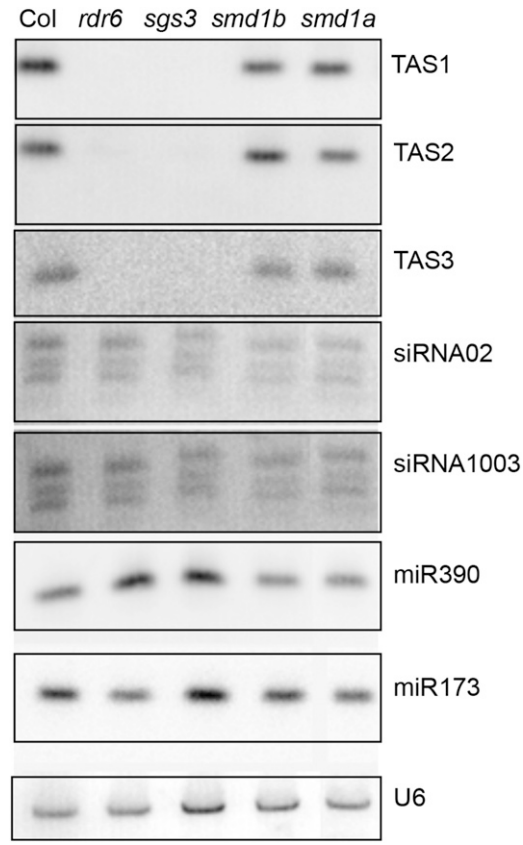

Figure 5. Endogenous Small RNA Accumulation in *smd1* Mutants.

RNA gel blot analysis of representative endogenous small RNAs in *smd1a* and *smd1b* mutants. Wild-type Col and *rdr6* and *sgs3* mutants are used as controls. *U6* snRNA hybridization served as loading controls for low molecular weight RNA gel blots.

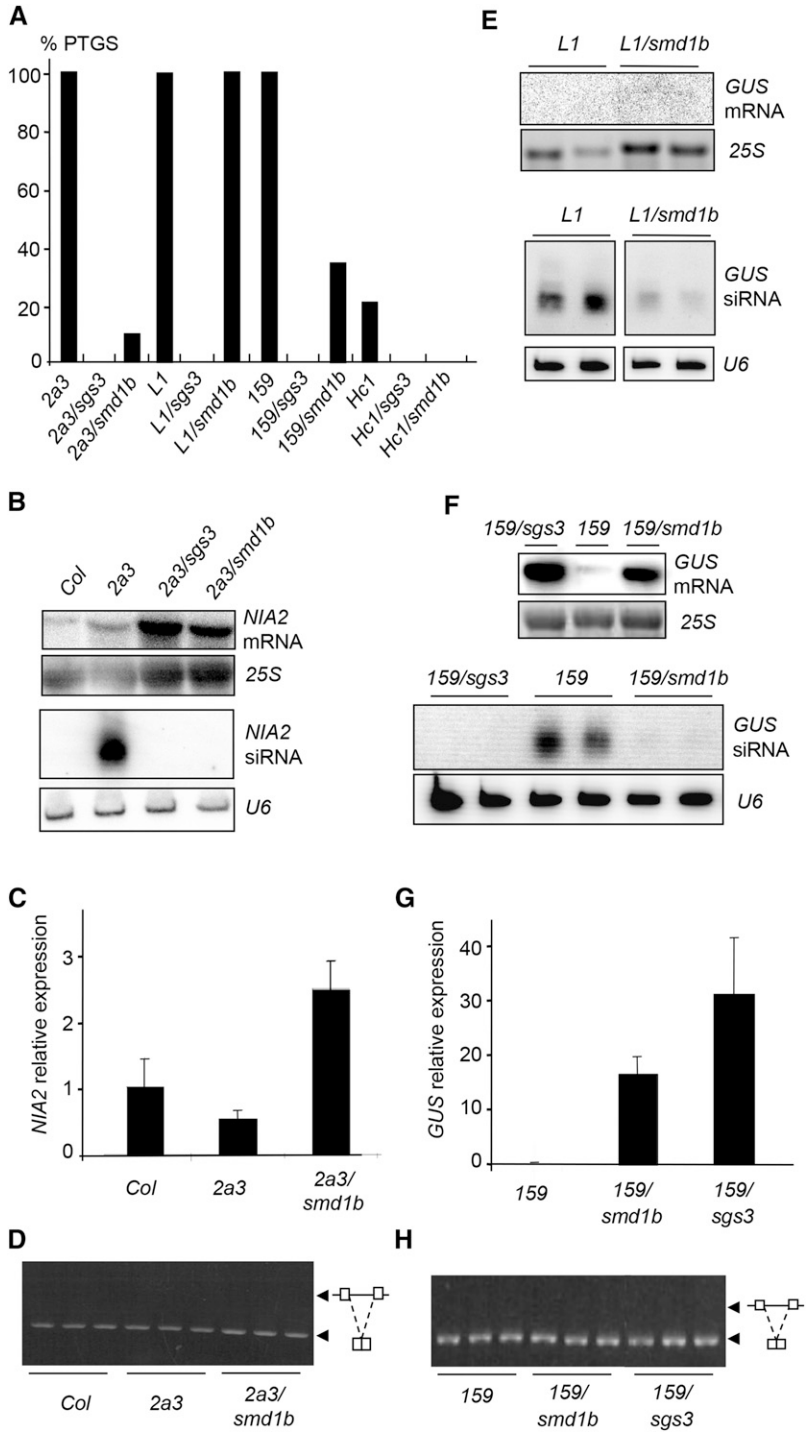

Figure 6. Transgene PTGS in *smd1b* Mutants.

(A) Percentages of silenced *2a3*, *L1*, *Hc1*, and *159* plants in the indicated genotypes determined by quantitative GUS activity measurements ($n = 96$ plants for each genotype).
(B) RNA gel blot analyses of *NIA* mRNA and siRNAs in the indicated genotypes.
(C) RT-qPCR quantification of mature *NIA2* mRNA in the indicated genotypes.
(D) Analysis of *NIA2* RNA splicing by RT-PCR using primers spanning an intron.
(E) RNA gel blot analyses of *L1 GUS* mRNA and siRNAs in the indicated genotypes.
(F) RNA gel blot analyses of *159 GUS* mRNA and siRNAs in the indicated genotypes.

transgene, the processing of the *2a3* and *159* pre-mRNAs was further analyzed to determine if the *smd1b* mutation causes transgene splicing defects that could affect PTGS. Unlike endogenous genes that exhibit intron retention in *smd1b* (Figure 4), the *2a3* and *159* transgenes did not show detectable changes in their splicing patterns (Figures 6D and 6H), suggesting that the *smd1b* does not compromise transgene splicing. Thus, PTGS impairment in *smd1b* does not appear to result from perturbed transgene splicing, suggesting that SmD1 acts in PTGS independent of its role in splicing.

To test this hypothesis, we attempted to determine if *smd1b* could affect PTGS of an intron-free transgene. To this end, we used the *Hc1* locus, which carries the very same *p35S:GUS* transgene as *L1*, but triggers *GUS* PTGS in only 20% of the population at each generation, whereas *L1* triggers *GUS* PTGS with 100% efficiency (Elmayan et al., 1998; Gy et al., 2007; Martínez de Alba et al., 2011, 2015). None of the *Hc1/smd1b* plants triggered *GUS* PTGS (Figure 6A), indicating that the *smd1b* mutation affects both *GUS* and *NIA2* PTGS. Altogether, these results indicate that the *smd1b* mutation abolishes PTGS of weak silencing lines (*Hc1*), reduces PTGS efficiency of medium-strength silencing lines (*2a3* and *159*), and only causes a reduction of siRNA accumulation in strong silencing lines (*L1*), which is insufficient to prevent PTGS.

SmD1b Binds to Pre-mRNA and mRNA Produced from Silenced Transgenes

The absence of a detectable effect of *smd1b* on the splicing of transgene RNA suggests that SmD1 facilitates PTGS independently of its role in splicing. To determine if SmD1 directly interacts with transgene RNA, the *159/smd1b* line was transformed with the *pUBQ10:SmD1b-GFP* construct, and complemented transformants that developed like wild-type plants and lacked GUS activity were selected. The nuclei extract (input) of the *159* line and one *159/smd1b/pUBQ10:Smd1b-GFP* transgenic line that triggered *GUS* PTGS as efficiently as the *159* line were used for RNA immunoprecipitation using anti-GFP antibodies to detect transgene RNAs bound to SMD1-GFP. Specific pairs of primers that amplify *GUS* pre-mRNA, *GUS* mRNA, or both forms (Figure 7A) were used to perform reverse transcription followed by quantitative real-time PCR on the RNA immunoprecipitation and input samples. The *NptII* gene that is adjacent to the *GUS* gene on the T-DNA was used as a nonsilenced control. Results indicate a strong enrichment of both *GUS* pre-mRNA and *GUS* mRNA, but not *NptII* mRNA (Figure 7B), indicating that SmD1 binds to RNAs produced by silenced transgenes but not from neighboring nonsilenced transgenes, thus supporting a direct role for SmD1 in PTGS.

Mutations in UPF3, XRN2, XRN3, or XRN4 RQC Factors Restore PTGS in *smd1b* Mutants

The results presented above suggest that SmD1 is not essential for PTGS but rather facilitates PTGS, in particular at weak silencing loci. Because RQC limits PTGS by degrading part of the transgene aberrant RNAs that provoke the activation of PTGS (Gy et al., 2007; Moreno et al., 2013; Lange et al., 2014; Martínez de Alba et al., 2015; Parent et al., 2015), we propose that SmD1 facilitates PTGS by limiting the degradation of transgene aberrant RNAs by the RQC machinery, thus favoring their entry into cytoplasmic siRNA bodies where they can trigger PTGS. To test this hypothesis, we crossed *159/smd1b* plants with various RQC-deficient mutants, including *mtr4*, *upf1*, *upf3*, *xrn2*, *xrn3*, and *xrn4*, to generate the corresponding double mutants. Remarkably, it was not possible to obtain viable *smd1b mtr4* double mutants. The siliques that formed on *smd1b/SmD1b mtr4/mtr4* or *smd1b/smd1b mtr4/MTR4* plants lacked 25% of the seeds, indicating that the *smd1b/smd1b mtr4/mtr4* double mutant is embryo-lethal. This result therefore suggests that SmD1 functions in the MTR4-dependent RQC pathway. In contrast, *smd1b upf1*, *smd1b upf3*, *smd1b xrn2*, *smd1b xrn3*, and *smd1b xrn4* double mutants were viable. However, the *upf1* and *159* loci were too close for obtaining plants carrying the *159* locus in a *smd1b upf1* background, thus limiting PTGS analysis to *smd1b upf3*, *smd1b xrn2*, *smd1b xrn3*, and *smd1b xrn4* double mutants. Whereas *GUS* PTGS occurred in 100% of *159* control plants and was reduced to 31% in *159/smd1b* mutant plants, it was restored to 100, 80, 90, and 100% in *smd1b upf3*, *smd1b xrn2*, *smd1b xrn3*, and *smd1b xrn4* plants, respectively (Figure 8A). Indeed, these plants accumulated *GUS* siRNA, whereas *159/smd1b* lacked *GUS* siRNA (Figure 8B), indicating that PTGS degrades *GUS* mRNA in these double mutants. These results demonstrate that PTGS can efficiently occur in the *smd1b* mutant, thus confirming that SmD1 is not part of the core PTGS machinery. Rather, they support the hypothesis that SmD1 facilitates PTGS by protecting transgene aberrant RNAs from degradation by the RQC machinery in the nucleus, thus increasing the amount of transgene aberrant RNAs that succeed to reach the cytoplasm. There aberrant RNAs still have to escape from cytoplasmic RQC (including XRN4) to enter siRNA bodies where they are transformed into dsRNA by RDR6, which eventually activates PTGS (Gy et al., 2007; Moreno et al., 2013; Lange et al., 2014; Martínez de Alba et al., 2015; Parent et al., 2015).

DISCUSSION

It has been hypothesized that transgene loci that produce large amounts of aberrant RNAs activate the PTGS pathway because these RNAs exceed the degradation capacity of the RQC pathways (Gy et al., 2007; Moreno et al., 2013; Lange et al., 2014;

Figure 6. (continued).

(G) RT-qPCR quantification of mature *GUS* mRNA in the indicated genotypes.

(H) Analysis of *GUS* RNA splicing by RT-PCR using primers spanning the intron.

25S rRNA hybridization or ethidium bromide staining served as loading controls for high molecular weight RNA gel blots. *U6* snRNA hybridization served as loading controls for low molecular weight RNA gel blots.

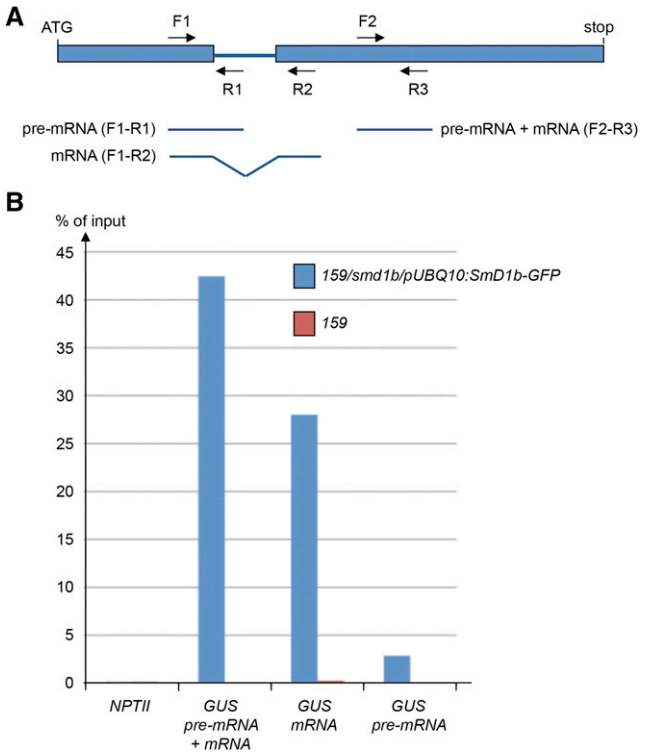

Figure 7. Transgene RNA Immunoprecipitation in *smd1b/pUBQ10:SmD1b-GFP* Plants.

(A) Schematic representation of the *GUS* RNA. Primers F1 + R1 specifically amplify *GUS* pre-mRNA. Primers F1+ R2 specifically amplify *GUS* mRNA. Primers F2 + R3 amplify both *GUS* pre-mRNA and mRNA.
(B) RNA immunoprecipitation using GFP antibodies, followed by RT and PCR using *GUS* and *NPTII* primers.

Martínez de Alba et al., 2015; Parent et al., 2015). Although this hypothesis probably holds true, it is possible that, in addition, cellular components protect aberrant RNAs from degradation by RQC, thus contributing to addressing larger amounts of these RNAs to the cytoplasm where they can activate PTGS. Our results suggest that the Arabidopsis nuclear ribonucleoprotein SmD1 facilitates PTGS by protecting transgene aberrant RNAs from degradation by the RQC machinery in the nucleus, thus increasing the amount of transgene aberrant RNAs that succeed to enter siRNA bodies in the cytoplasm to eventually activate PTGS.

SmD1 is encoded by two closely related although differentially expressed genes. Both *smd1a* and *smd1b* single mutants are viable, but the double mutant cannot be obtained, indicating that SmD1 function is essential for the plant. Consistent with their expression level, *SmD1b* is more important than *SmD1a* because *smd1b* but not *smd1a* mutants exhibit developmental defects. Moreover, *smd1a/smd1a smd1b/SmD1B* plants exhibit developmental defects milder than those of the *smd1b* homozygous mutant, whereas *smd1a/SmD1a smd1b/smd1b* cannot be identified, indicating that either one copy of *SmD1b* or two copies of *SmD1a* is necessary for the plant to survive. Lastly, both *pUBQ10:SmD1b* and *pUBQ10:SmD1a* constructs restored wild-type development when introduced in *smd1b*, indicating that SmD1a and SmD1b proteins have redundant activity. In yeast, SmD1 participates in stabilizing RNA-RNA interactions between the 5′ end of the U1 small nuclear RNA and the 5′ splice sites of pre-mRNA substrates (Zhang et al., 2001). We found that Arabidopsis SmD1 colocalizes with the splicing factor SR34 in nucleoplasmic speckles, suggesting that SmD1 also participates in splicing in plants. Even though no global defects in mRNA splicing were found, intron retention at certain endogenous genes was observed in the *smd1b* mutant. Given the redundant function of SmD1a and SmD1b, it is possible that the *smd1a smd1b* double mutant is lethal because of splicing defects in essential genes.

SmD1 also localizes in the nucleolus, suggesting additional functions besides splicing. Attempts to obtain double mutants between *smd1b* and *mtr4*, *upf3*, or *xrn2* mutants impaired in RQC components that also reside in the nucleolus revealed that the *smd1b mtr4* double mutant is embryo-lethal, whereas *smd1b upf3* and *smd1b xrn2* double mutants are viable. MTR4 acts in the nucleolar exosome (Lange et al., 2014). Whether SmD1 associates with the nucleolar exosome remains to be determined, but this result suggests that, in addition to splicing, SmD1 could play a role in MTR4-dependent RQC function in the nucleolus.

How does SmD1 affect PTGS, and is the effect of SmD1 on PTGS related to its splicing function? Although mutations in the putative splicing factor ESP3/PRP2 were identified in a screen for enhanced PTGS (Herr et al., 2006), very little is known about possible links between splicing and PTGS. Intron-free transgenes appear more prone to trigger PTGS than intron-containing transgenes (Christie et al., 2011), suggesting that the splicing process and/or the splicing machinery somehow protects RNA from entering into the PTGS pathway. The fact that the splicing factor SmD1 facilitates PTGS is somehow inconsistent with these two reports, asking whether SmD1 could affect PTGS indirectly through the deregulation of components of the PTGS machinery. However, PTGS occurs efficiently in *smd1b upf3*, *smd1b xrn2*, *smd1b xrn3*, and *smd1b xrn4* double mutants, indicating that the *smd1b* mutation does not compromise the splicing of a component of the PTGS machinery. Moreover, no detectable effect of the *smd1b* mutation on the splicing of transgene RNA was observed, suggesting that SmD1 facilitates PTGS through a mechanism that is independent of its role in splicing. Supporting this hypothesis, we found that the *smd1b* mutation affects PTGS triggered by both intron-containing and intron-free transgenes. Finally, we found that SmD1b binds to both pre-mRNA and mRNA produced by silenced transgenes but not by nonsilenced transgenes, strongly suggesting a direct role in facilitating PTGS independent of splicing.

A facilitating role rather than an essential role in PTGS is supported by the fact that the *smd1b* mutation does not prevent transgene PTGS triggered by the strong inducing line *L1* (which triggers PTGS with 100% efficiency), reduces PTGS triggered by lines *159* and *2a3* (which also trigger PTGS with 100% efficiency but at a slower rate than *L1*), and abolishes PTGS triggered by the weak inducing line *Hc1* (which only triggers PTGS with 20% efficiency). Although we cannot exclude that the *smd1a smd1b* double mutation could completely abolish PTGS in *L1*, *159*, and *2a3* lines, these results suggest that SmD1 facilitates PTGS triggered by weak inducers, but is dispensable for PTGS triggered by strong inducers. We propose that SmD1 participates in the PTGS of weak inducers by limiting the degradation of transgene aberrant RNAs by

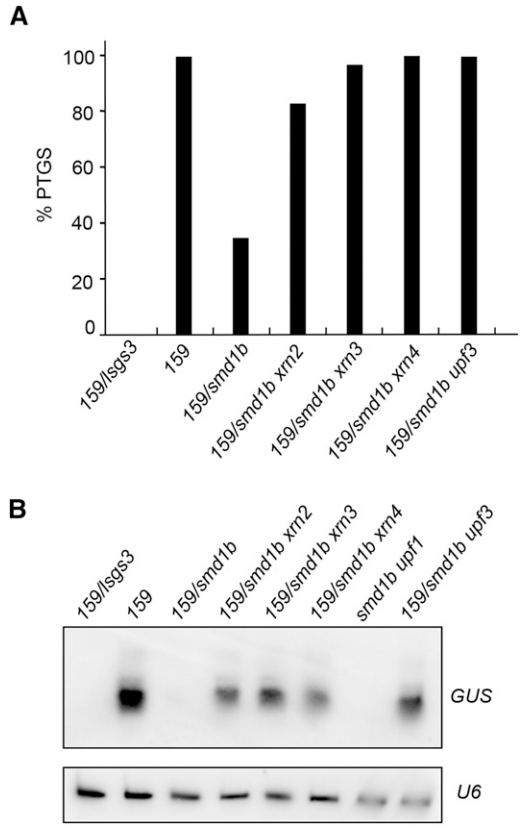

Figure 8. PTGS and siRNA Accumulation in Double Mutants Involving *smd1b*.

(A) Percentages of plants silenced by PTGS in the indicated genotypes determined by quantitative GUS activity measurements (n = 96 plants for each genotype).

(B) RNA gel blot analyses of *GUS* siRNAs in the indicated genotypes. *U6* snRNA hybridization served as a loading control. Note that the *sm1d upf1* double mutant does not contain the *159* locus because *upf1* and *159* loci are very close.

RQC in the nucleus, thus facilitating their addressing to the cytoplasm where they need to enter into siRNA bodies to activate PTGS. If this hypothesis is correct, SmD1 should not be part of the core PTGS machinery, and PTGS should still operate in *smd1b* mutants if large amounts of transgene aberrant RNAs are produced or if RQC is compromised. This is exactly what happens in the strong silencing line *L1*. PTGS likely occurs in *L1/smd1b* plants because *L1* produces very high amounts of transgene aberrant RNAs, which exceed the capacity of the RQC pathways. Even if part of the transgene aberrant RNAs produced by *L1* is degraded by RQC pathways, the amount that remains is probably sufficient to enter the PTGS pathway without the requirement of SmD1. Also consistent with our hypothesis, we observed that PTGS of line *159*, which was strongly reduced in *smd1b*, was restored to wild-type levels in *smd1b upf3*, *smd1b xrn2*, *smd1b xrn3*, and *smd1b xrn4* double mutants, confirming that the *smd1b* mutation does not impair the functioning of the PTGS machinery. Rather, transgene aberrant RNAs, which are less abundant in 159 than in L1, likely are more efficiently degraded by nuclear RQC in the absence of SmD1, thus limiting the triggering of PTGS. Only in double mutants between *smd1b* and either *upf3*, *xrn2*, *xrn3*, or *xrn4*, the impairment of one or the other RQC component limits the degradation of transgene aberrant RNAs, allowing a sufficient amount to reach siRNA bodies in the cytoplasm to trigger PTGS.

To summarize, the impairment of PTGS in *smd1b* and the reestablishment of PTGS in double mutants between *smd1b* and several RQC-deficient mutants suggest that, in addition to its role in splicing, SmD1 facilitates PTGS by limiting the degradation of transgene aberrant RNAs by nuclear RQC, revealing new roles for the SmD1 splicing regulator in RQC and PTGS. Because the role of SmD1 in splicing involves stabilizing weak RNA-RNA interactions between U1 small nuclear RNA and pre-mRNA splicing substrates (Zhang et al., 2001), it is possible that the role of SmD1 in PTGS also involves the stabilization of weak RNA-RNA interactions. In the case of PTGS, RNA-RNA interactions that need to be stabilized could involve secondary structures within aberrant RNAs, which need to be protected to prevent degradation by RQC components and favor RNA export to the cytoplasm.

METHODS

Plant Material and Growth Conditions

All *Arabidopsis thaliana* plants are in the Columbia accession. Transgenic lines *2a3*, *L1*, and *Hc1* and mutants *mtr4-2*, *sgs3-1*, *upf1-6*, *upf3-3*, *xrn2-2*, *xrn3-3*, and *xrn4-5* were previously described (Elmayan et al., 1998; Mourrain et al., 2000; Gy et al., 2007; Moreno et al., 2013; Lange et al., 2014). The *smd1a* T-DNA insertion mutant SALK_024397 was obtained from NASC (Alonso et al., 2003). Line *159* was produced during this study by screening lines undergoing PTGS among the homozygous progeny of Arabidopsis transformants carrying the same *p35S:GUS* transgene as in lines *L1* and *Hc1* except for the addition of a plant intron (Vancanneyt et al., 1990). Plants were grown on Bouturage media (Duchefa) in standard long-day conditions (16 h light, 8 h dark at 20 to 22°C), transferred to soil after 2 weeks, and grown in controlled growth chambers in standard long-day conditions.

Plasmid Constructs

The *pSmD1b:SmD1b* construct was generated as follows: a 2943-bp genomic fragment starting 1 kb upstream the ATG of At4g02840 and ending 500 bp downstream its stop codon was amplified with Phusion High-fidelity DNA polymerase (Thermo) using primers SmD1b-1 and SmD1b-2, which carry *Hind*III and *Eco*RI sites at their ends, respectively (Supplemental Table 1). After cloning in TOPO blunt-end vector (Life Technologies) and verification by sequencing, the *Hind*III-*Eco*RI insert was subcloned in the binary pBINplus vector (van Engelen et al., 1995).

The *pUBQ10:SmD1a*, *pUBQ10:SmD1b*, *pUBQ10:SmD1a-GFP*, and *pUBQ10:SmD1b-GFP* constructs were made using Gateway technology (Invitrogen) as follows. For SmD1b, a 1621-bp genomic fragment starting 96 bp upstream the ATG of At4g02840 and ending at the stop codon was amplified with Phusion High-Fidelity DNA polymerase (Thermo) using primers SmD1b-3 and SmD1b-4 (Supplemental Table 1). After recombination into pENTR/D vector through the Gateway BP recombinase reaction (Invitrogen) and verification by sequencing, final recombination into pUB-DEST and pUBC-GFP through the Gateway LR recombinase reaction (Invitrogen) created *pUBQ10:SmD1b* and *pUBQ10:SmD1b-GFP*, respectively. For SmD1a, a 863-bp genomic fragment starting 53 bp upstream the ATG of At3g07590 and ending at the stop codon was amplified with Phusion High-Fidelity DNA polymerase (Thermo) using primers

SmD1a-1 and SmD1a-2 (Supplemental Table 1). After recombination into pDONR-207 vector through the gateway BP recombinase reaction (Invitrogen) and verification by sequencing, final recombination into pUB-DEST and pUBC-GFP through the Gateway LR recombinase reaction (Invitrogen) created *pUBQ10:SmD1a* and *pUBQ10:SmD1a-GFP*, respectively.

The *p35S:SR34-RFP*, *p35S:UPF3-RFP*, and *p35S:XRN2-RFP* constructs have been described previously (Lorković et al., 2008; Moreno et al., 2013).

Arabidopsis Transformation and *Nicotiana benthamiana* Agroinfiltration

Agrobacterium strains carrying plasmids of interest were grown overnight at 28°C in 3 mL Luria-Bertani medium containing the appropriate antibiotics to a final OD_{600} between 1 and 2. For Arabidopsis transformation, the bacteria were pelleted and resuspended in 300 mL of infiltration medium (5% sucrose, 10 mM $MgCl_2$, and 0.015% Silwet L-77) to a final OD_{600} of 1, which was used for floral dipping. For *N. benthamiana* agroinfiltration, the bacteria were pelleted and resuspended in 1 mL of infiltration medium (10 mM $MgCl_2$, 10 mM MES, pH 5.2, and 150 mM acetosyringone) to a final OD_{600} of 0.1. The solution containing the bacteria was injected into the abaxial side leaves using a 1-mL syringe and samples were observed in a confocal microscope 3 d after infiltration.

Imaging and Image Analysis

After agroinfiltration, fluorescent cells were imaged by confocal microscopy (Leica TCS SP2; Leica Microsystems) with excitation at 488 nm and fluorescence emission signal between 495 and 530 nm for GFP fusions, and excitation at 543 nm and emission signal between 555 and 620 nm for DsRed or RFP fusions. The Leica confocal software was used for image acquisition and for the quantification of fluorescence profiles. Sequential scans were performed when necessary. Spectral profiles were calculated for five cells. Data processing was performed using ImageJ (http://rsbweb.nih.gov/ij/).

RNA Extraction and RNA Gel Blot Analysis

For RNA gel blot analyses, frozen tissue was homogenized in a buffer containing 0.1 M NaCl, 2% SDS, 50 mM Tris-HCl, pH 9.0, 10 mM EDTA, pH 8.0, and 20 mM β-mercaptoethanol and RNAs were extracted two times with phenol and recovered by ethanol precipitation. To obtain high molecular weight RNA fraction, resuspended RNAs were precipitated overnight in 2 M LiCl at 4°C and recovered by centrifugation. For low molecular weight RNA analysis, total RNA was separated on a 15% denaturing PAGE gel, stained with ethidium bromide, and transferred to nylon membrane (HybondNX; Amersham). Low molecular weight RNA and U6 hybridizations were at 50°C with hybridization buffer containing 5× SSC, 20 mM Na_2HPO_4, pH 7.2, 7% SDS, 2× Denhardt's solution, and denatured sheared salmon sperm DNA (Invitrogen). High molecular weight RNA hybridization was at 37°C in PerfectHyb Plus buffer (Sigma-Aldrich). Blots were hybridized with a radioactively labeled random-primed DNA probes for *GUS* mRNA and *GUS* siRNAs and an end-labeled oligonucleotide probe for U6 detection.

RT-PCR Analysis

Total RNA was prepared from roots and plantlets at different developmental stages using the Qiagen RNeasy plant mini kit. The DNase treatment was performed according to the manufacturer's protocols. For reverse transcription with SuperScript II (Invitrogen), 2.5 μg of total DNase-treated RNA was used. One microliter of the resulting cDNA solution was used for RT-PCR or RT-qPCR analyses. The latter was done using standard protocols and a complete list of RT-qPCR primers is available in Supplemental Table 1. Each cDNA sample was precisely calibrated and verified for two constitutive genes, AT1G13320 and AT4G26410 (Czechowski et al., 2005). For RT-PCR, the amplification was performed as follows: one cycle of 4 min at 98°C, 26 cycles of 30 s at 98°C, 30 s at 59°C, and 1 min at 72°C. The products were separated on a 7.5% polyacrylamide gel stained with SyBr green (Invitrogen) and revealed by Pharos Imager (Bio-Rad). Band profiles were quantified using ImageJ (http://rsbweb.nih.gov/ij/). RT-qPCR was performed using a Roche Light Cycler 480 standard protocol (40 cycles, 60°C annealing).

RNA Immunoprecipitation

Eleven-day-old plants grown in Petri dishes were irradiated three times with UV using a CL-508 cross-linker (Uvitec) at 0.400 J/cm^2. Briefly, fixed material was ground in liquid nitrogen and homogenized and nuclei isolated and lysed according to Gendrel et al. (2005). RNA immunoprecipitation was basically performed as described by Carlotto et al. (2016). The nuclei extract (input) was used for the immunoprecipitation performed by the Direct ChIP Protocol of the Diagenode IP-Star SX-86 Compact robot, using 50 μL of Dynabeads-Protein A (Novex 10008D; Life Technologies) and anti-GFP antibodies (632381; Clontech). Beads were washed twice for 5 min at 4°C with wash buffer 1 (150 mM NaCl, 1% Triton, 0.5% Nonidet P-40, 1 mM EDTA, and 20 mM Tris-HCl, pH7.5) and twice with wash buffer 2 (20 mM Tris-HCl, pH 8) instead of the Diagenode assigned buffers and finally resuspended in 100 μL Proteinase K buffer (100 mM Tris-HCl, pH 7.4, 50 mM NaCl, and 10 mM EDTA). After Proteinase K (AM2546; Ambion) treatment, beads were removed with a magneto, and the supernatants were transferred to a 2-mL tube. Each RNA sample was extracted from 800 μL (8 IP-Star tubes) of RNA immunoprecipitation product using 1 mL of TriReagent (Sigma-Aldrich T9424) as indicated by the manufacturer. Eighty microliters of nuclei extracts was used for input RNA extraction. The immunoprecipitation and input samples were treated with DNase, and random hexamers were used for subsequent RT. Quantitative real-time PCR reactions were performed using specific primers. Results were expressed as a percentage of cDNA detected after immunoprecipitation, taking the input sample as 100%.

GUS Extraction and Activity Quantification

GUS protein was extracted and GUS activity was quantified as described before (Gy et al., 2007) from cauline leaves of flowering plants by measuring the quantity of 4-methylumbelliferone product generated from the substrate 4-methylumbelliferyl-β-D-glucuronide (Duchefa) on a fluorometer (Fluoroscan II; Thermo Scientific).

Accession Numbers

Sequence data from this article can be found in the GenBank/EMBL libraries under the following accession numbers: SmD1b (At4g02840) and SmD1a (At3g07590).

Supplemental Data

Supplemental Figure 1. Original blot for Figure 6E.

Supplemental Table 1. Primers used in this study.

ACKNOWLEDGMENTS

We thank T. Elmayan for helpful discussions and P. Grillot, H. Ferry, and P. Marechal for plant care. This work was supported by the Agence Nationale de la Recherche ANR-10-BLAN-1707 (to H.V.) and ANR-10-LABX-40 (to M.D.C. and H.V.).

AUTHOR CONTRIBUTIONS

H.V. and M.D.C. designed the experiments. All authors contributed to the production and analysis of the results. H.V. wrote the article with contribution from all the other authors.

Received December 18, 2015; revised January 29, 2016; accepted January 29, 2016; published February 3, 2016.

REFERENCES

Alonso, J.M., et al. (2003). Genome-wide insertional mutagenesis of *Arabidopsis thaliana*. Science **301:** 653–657.

Baulcombe, D. (2004). RNA silencing in plants. Nature **431:** 356–363.

Baumberger, N., and Baulcombe, D.C. (2005). Arabidopsis ARGONAUTE1 is an RNA Slicer that selectively recruits microRNAs and short interfering RNAs. Proc. Natl. Acad. Sci. USA **102:** 11928–11933.

Boutet, S., Vazquez, F., Liu, J., Béclin, C., Fagard, M., Gratias, A., Morel, J.B., Crété, P., Chen, X., and Vaucheret, H. (2003). Arabidopsis HEN1: a genetic link between endogenous miRNA controlling development and siRNA controlling transgene silencing and virus resistance. Curr. Biol. **13:** 843–848.

Cao, J., Shi, F., Liu, X., Jia, J., Zeng, J., and Huang, G. (2011). Genome-wide identification and evolutionary analysis of Arabidopsis sm genes family. J. Biomol. Struct. Dyn. **28:** 535–544.

Carlotto, N., Wirth, S., Furman, N., Ferreyra Solari, N., Ariel, F., Crespi, M., and Kobayashi, K. (2016). The chloroplastic DEVH-box RNA helicase INCREASED SIZE EXCLUSION LIMIT 2 involved in plasmodesmata regulation is required for group II intron splicing. Plant Cell Environ. **39:** 165–173.

Christie, M., Croft, L.J., and Carroll, B.J. (2011). Intron splicing suppresses RNA silencing in Arabidopsis. Plant J. **68:** 159–167.

Czechowski, T., Stitt, M., Altmann, T., Udvardi, M.K., and Scheible, W.R. (2005). Genome-wide identification and testing of superior reference genes for transcript normalization in Arabidopsis. Plant Physiol. **139:** 5–17.

Elmayan, T., Balzergue, S., Béon, F., Bourdon, V., Daubremet, J., Guénet, Y., Mourrain, P., Palauqui, J.C., Vernhettes, S., Vialle, T., Wostrikoff, K., and Vaucheret, H. (1998). Arabidopsis mutants impaired in cosuppression. Plant Cell **10:** 1747–1758.

Fagard, M., Boutet, S., Morel, J.B., Bellini, C., and Vaucheret, H. (2000). AGO1, QDE-2, and RDE-1 are related proteins required for post-transcriptional gene silencing in plants, quelling in fungi, and RNA interference in animals. Proc. Natl. Acad. Sci. USA **97:** 11650–11654.

Gazzani, S., Lawrenson, T., Woodward, C., Headon, D., and Sablowski, R. (2004). A link between mRNA turnover and RNA interference in Arabidopsis. Science **306:** 1046–1048.

Gendrel, A.V., Lippman, Z., Martienssen, R., and Colot, V. (2005). Profiling histone modification patterns in plants using genomic tiling microarrays. Nat. Methods **2:** 213–218.

Golisz, A., Sikorski, P.J., Kruszka, K., and Kufel, J. (2013). *Arabidopsis thaliana* LSM proteins function in mRNA splicing and degradation. Nucleic Acids Res. **41:** 6232–6249.

Gy, I., Gasciolli, V., Lauressergues, D., Morel, J.B., Gombert, J., Proux, F., Proux, C., Vaucheret, H., and Mallory, A.C. (2007). Arabidopsis FIERY1, XRN2, and XRN3 are endogenous RNA silencing suppressors. Plant Cell **19:** 3451–3461.

Hernandez-Pinzon, I., Yelina, N.E., Schwach, F., Studholme, D.J., Baulcombe, D., and Dalmay, T. (2007). SDE5, the putative homologue of a human mRNA export factor, is required for transgene silencing and accumulation of trans-acting endogenous siRNA. Plant J. **50:** 140–148.

Herr, A.J., Molnàr, A., Jones, A., and Baulcombe, D.C. (2006). Defective RNA processing enhances RNA silencing and influences flowering of Arabidopsis. Proc. Natl. Acad. Sci. USA **103:** 14994–15001.

Jauvion, V., Elmayan, T., and Vaucheret, H. (2010). The conserved RNA trafficking proteins HPR1 and TEX1 are involved in the production of endogenous and exogenous small interfering RNA in Arabidopsis. Plant Cell **22:** 2697–2709.

Lange, H., et al. (2014). The RNA helicases AtMTR4 and HEN2 target specific subsets of nuclear transcripts for degradation by the nuclear exosome in *Arabidopsis thaliana*. PLoS Genet. **10:** e1004564.

Le Masson, I., Jauvion, V., Bouteiller, N., Rivard, M., Elmayan, T., and Vaucheret, H. (2012). Mutations in the Arabidopsis H3K4me2/3 demethylase JMJ14 suppress posttranscriptional gene silencing by decreasing transgene transcription. Plant Cell **24:** 3603–3612.

Li, J., Yang, Z., Yu, B., Liu, J., and Chen, X. (2005). Methylation protects miRNAs and siRNAs from a 3′-end uridylation activity in Arabidopsis. Curr. Biol. **15:** 1501–1507.

Lorković, Z.J., Hilscher, J., and Barta, A. (2008). Co-localisation studies of Arabidopsis SR splicing factors reveal different types of speckles in plant cell nuclei. Exp. Cell Res. **314:** 3175–3186.

Martínez de Alba, A.E., Elvira-Matelot, E., and Vaucheret, H. (2013). Gene silencing in plants: a diversity of pathways. Biochim. Biophys. Acta **1829:** 1300–1308.

Martínez de Alba, A.E., Jauvion, V., Mallory, A.C., Bouteiller, N., and Vaucheret, H. (2011). The miRNA pathway limits AGO1 availability during siRNA-mediated PTGS defense against exogenous RNA. Nucleic Acids Res. **39:** 9339–9344.

Martínez de Alba, A.E., Moreno, A.B., Gabriel, M., Mallory, A.C., Christ, A., Bounon, R., Balzergue, S., Aubourg, S., Gautheret, D., Crespi, M.D., Vaucheret, H., and Maizel, A. (2015). In plants, decapping prevents RDR6-dependent production of small interfering RNAs from endogenous mRNAs. Nucleic Acids Res. **43:** 2902–2913.

Morel, J.B., Godon, C., Mourrain, P., Béclin, C., Boutet, S., Feuerbach, F., Proux, F., and Vaucheret, H. (2002). Fertile hypomorphic ARGONAUTE (ago1) mutants impaired in post-transcriptional gene silencing and virus resistance. Plant Cell **14:** 629–639.

Moreno, A.B., Martínez de Alba, A.E., Bardou, F., Crespi, M.D., Vaucheret, H., Maizel, A., and Mallory, A.C. (2013). Cytoplasmic and nuclear quality control and turnover of single-stranded RNA modulate post-transcriptional gene silencing in plants. Nucleic Acids Res. **41:** 4699–4708.

Mourrain, P., et al. (2000). Arabidopsis SGS2 and SGS3 genes are required for posttranscriptional gene silencing and natural virus resistance. Cell **101:** 533–542.

Parent, J.S., Jauvion, V., Bouche, N., Beclin, C., Hachet, M., Zytnicki, M., and Vaucheret, H. (2015). Post-transcriptional gene silencing triggered by sense transgenes involves uncapped antisense RNA and differs from silencing intentionally triggered by antisense transgenes. Nucleic Acids Res. **43:** 8464–8475.

Perea-Resa, C., Hernández-Verdeja, T., López-Cobollo, R., del Mar Castellano, M., and Salinas, J. (2012). LSM proteins provide accurate splicing and decay of selected transcripts to ensure normal Arabidopsis development. Plant Cell **24:** 4930–4947.

Simpson, C.G., Fuller, J., Maronova, M., Kalyna, M., Davidson, D., McNicol, J., Barta, A., and Brown, J.W. (2008). Monitoring changes in alternative precursor messenger RNA splicing in multiple gene transcripts. Plant J. **53:** 1035–1048.

Thran, M., Link, K., and Sonnewald, U. (2012). The Arabidopsis DCP2 gene is required for proper mRNA turnover and prevents transgene silencing in Arabidopsis. Plant J. **72:** 368–377.

Vancanneyt, G., Schmidt, R., O'Connor-Sanchez, A., Willmitzer, L., and Rocha-Sosa, M. (1990). Construction of an intron-containing marker gene: splicing of the intron in transgenic plants and its use in monitoring early events in Agrobacterium-mediated plant transformation. Mol. Gen. Genet. **220:** 245–250.

van Engelen, F.A., Molthoff, J.W., Conner, A.J., Nap, J.P., Pereira, A., and Stiekema, W.J. (1995). pBINPLUS: an improved plant transformation vector based on pBIN19. Transgenic Res. **4:** 288–290.

Voinnet, O. (2009). Origin, biogenesis, and activity of plant microRNAs. Cell **136:** 669–687.

Wang, B.B., and Brendel, V. (2004). The ASRG database: identification and survey of Arabidopsis thaliana genes involved in pre-mRNA splicing. Genome Biol. **5:** R102.

Yelina, N.E., Smith, L.M., Jones, A.M., Patel, K., Kelly, K.A., and Baulcombe, D.C. (2010). Putative Arabidopsis THO/TREX mRNA export complex is involved in transgene and endogenous siRNA biosynthesis. Proc. Natl. Acad. Sci. USA **107:** 13948–13953.

Yu, A., Saudemont, B., Bouteiller, N., Elvira-Matelot, E., Lepère, G., Parent, J.S., Morel, J.B., Cao, J., Elmayan, T., and Vaucheret, H. (2015). Second-site mutagenesis of a hypomorphic argonaute1 allele identifies SUPERKILLER3 as an endogenous suppressor of transgene posttranscriptional gene silencing. Plant Physiol. **169:** 1266–1274.

Zhang, D., Abovich, N., and Rosbash, M. (2001). A biochemical function for the Sm complex. Mol. Cell **7:** 319–329.